Enhanced Contrast Source Inversion Using Multi-Resolution BCS

M. Salucci, L. Poli, F. Zardi, L.Tosi, S. Lusa, and A. Massa

2025/04/04

Contents

1 Numerical Results: Hollow Square, $\ell = 1.5\lambda$

Test Case Description

Direct solver:

- Side of the investigation domain: $L = 6.0\lambda$
- Cubic domain divided in $\sqrt{D} \times \sqrt{D}$ cells
- Number of cells for the direct solver: $D = 1600$ (discretization $= \lambda/10$)

Investigation domain:

- Cubic domain divided in $\sqrt{N} \times \sqrt{N}$ cells
- Number of cells for the inversion:

  - First Step IMSA: $N^{(1)} = 100$ (discretization $= \lambda/10$)

  - Following Steps IMSA: $N^{(i)}$ not fixed, defined according to the estimated *RoI* $\mathcal{D}^{(i)}$

Measurement domain:

- Total number of measurements: $M = 60$
- Measurement points placed on circles of radius $\rho = 4.5\lambda$

Sources:

- Plane waves
- Number of views: $V = 60$; $\theta_{inc}^{v} = 0 + (v-1) \times (360/V)$
- Amplitude: $A = 1.0$
- Frequency: $F = 300$ MHz ($\lambda = 1$)

Background:

- $\varepsilon_r = 1.0$
- $\sigma = 0$ [S/m]

Scatterer

- Hollow square object, $\ell = 1.5\lambda$
- $\varepsilon_r \in \{1.05,\ 1.10,\ 1.15, 1.20,\ 1.25,\ 1.50,\ 2.00,\ 2.50\}$
- $\sigma = 0$ [S/m]

1.0.1 Hollow Square, $\ell = 1.5\lambda$, $\tau = 0.10$ - IMSA-BCS reconstructed profiles

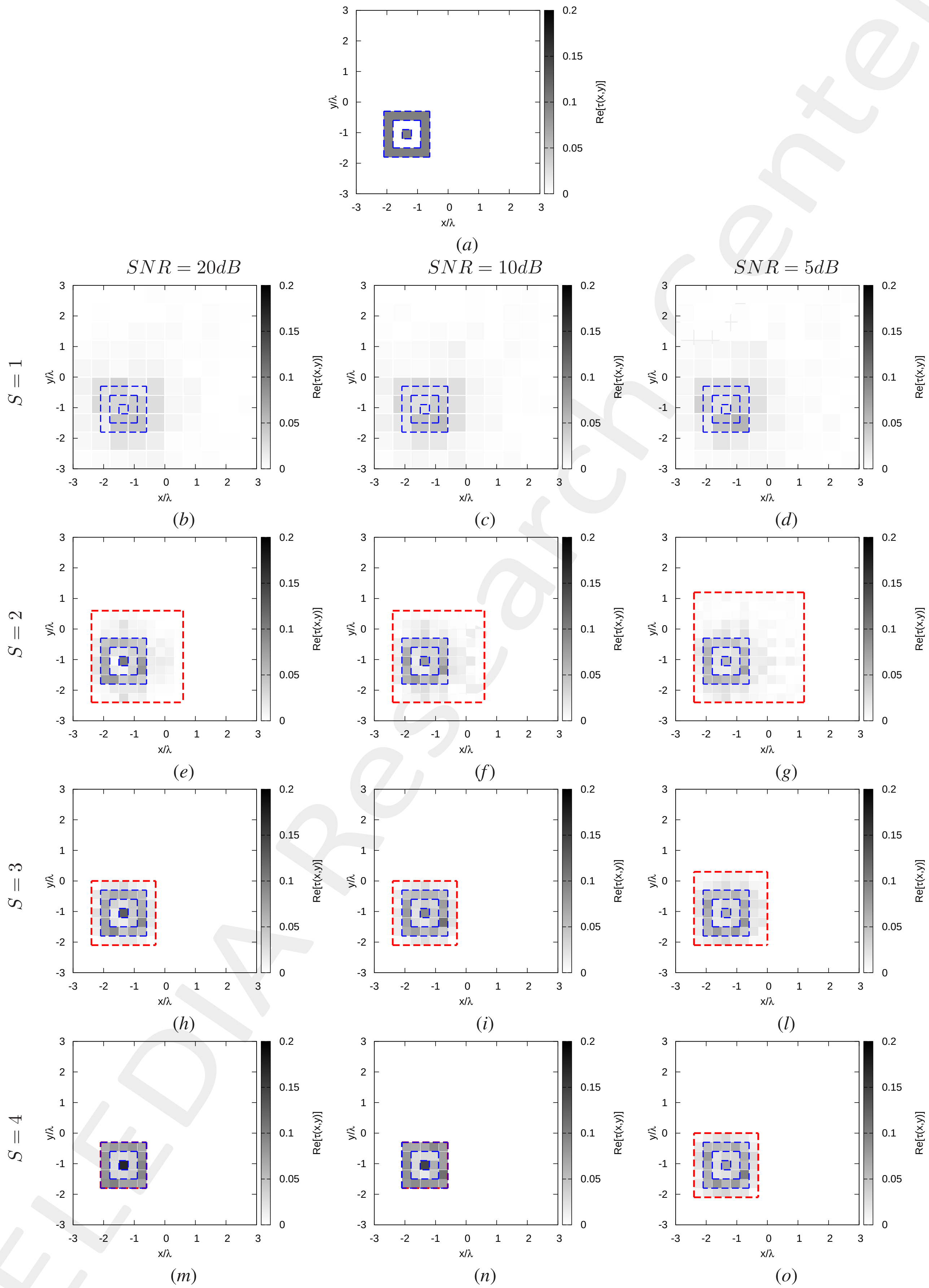

Figure 1: *Hollow Square*, $\ell = 1.5\lambda$, $\tau = 0.10$ - (a) Actual profile and (b)-(o) IMSA-BCS reconstructed profiles for $(b)(e)(h)(m)$ $SNR = 20$ [dB], $(c)(f)(i)(n)$ $SNR = 10$ [dB] and $(d)(g)(l)(o)$ $SNR = 5$ [dB] at the step (b)-(d) $S = 1$, (e)-(g) $S = 2$, (h)-(l) $S = 3$ and (m)-(o) $S = 4$.

	$SNR = 50dB$			
	$S=1$	$S=2$	$S=3$	$S=4$
ξ_{tot}	7.89×10^{-3}	3.43×10^{-3}	2.79×10^{-3}	1.58×10^{-3}
ξ_{int}	6.10×10^{-2}	3.77×10^{-2}	3.27×10^{-2}	2.17×10^{-2}
ξ_{ext}	5.34×10^{-3}	1.83×10^{-3}	1.41×10^{-3}	6.33×10^{-4}
	$SNR = 20dB$			
	$S=1$	$S=2$	$S=3$	$S=4$
ξ_{tot}	7.95×10^{-3}	3.42×10^{-3}	2.77×10^{-3}	1.56×10^{-3}
ξ_{int}	6.11×10^{-2}	3.67×10^{-2}	3.12×10^{-2}	2.00×10^{-2}
ξ_{ext}	5.37×10^{-3}	1.85×10^{-3}	1.47×10^{-3}	6.82×10^{-4}
	$SNR = 10dB$			
	$S=1$	$S=2$	$S=3$	$S=4$
ξ_{tot}	7.90×10^{-3}	3.73×10^{-3}	2.93×10^{-3}	1.56×10^{-3}
ξ_{int}	5.89×10^{-2}	3.98×10^{-2}	3.16×10^{-2}	1.94×10^{-2}
ξ_{ext}	5.33×10^{-3}	2.04×10^{-3}	1.60×10^{-3}	7.20×10^{-4}
	$SNR = 5dB$			
	$S=1$	$S=2$	$S=3$	$S=4$
ξ_{tot}	8.06×10^{-3}	4.38×10^{-3}	3.54×10^{-3}	3.15×10^{-3}
ξ_{int}	5.78×10^{-2}	4.50×10^{-2}	3.73×10^{-2}	3.28×10^{-2}
ξ_{ext}	5.44×10^{-3}	2.40×10^{-3}	1.97×10^{-3}	1.75×10^{-3}

Table I: *Hollow Square*, $\ell = 1.5\lambda$, $\tau = 0.10$ - Reconstrution errors: total (ξ_{tot}), internal (ξ_{int}) and external (ξ_{ext}) errors.

	$SNR = 50dB$			
	$S=1$	$S=2$	$S=3$	$S=4$
$L^{(S)}$	6.00	1.50	1.50	1.50
$N^{(S)}$	100	175	175	175
$Q^{(S)}$	100	100	49	25
	$SNR = 20dB$			
	$S=1$	$S=2$	$S=3$	$S=4$
$L^{(S)}$	6.00	1.50	1.50	1.50
$N^{(S)}$	100	175	175	175
$Q^{(S)}$	100	100	49	25
	$SNR = 10dB$			
	$S=1$	$S=2$	$S=3$	$S=4$
$L^{(S)}$	6.00	1.50	1.50	1.50
$N^{(S)}$	100	175	175	175
$Q^{(S)}$	100	100	49	25
	$SNR = 5dB$			
	$S=1$	$S=2$	$S=3$	$S=4$
$L^{(S)}$	6.00	2.10	1.80	1.80
$N^{(S)}$	100	208	208	208
$Q^{(S)}$	100	144	64	49

Table II: *Hollow Square*, $\ell = 1.5\lambda$, $\tau = 0.10$ - Investigation domain parameters: restricted investigation domain size $L^{(S)}$, total number of cells $N^{(S)}$ and number of cells within the restricted domain size $Q^{(S)}$.

1.0.2 Hollow Square, $\ell = 1.5\lambda$, $\tau = 0.20$ - IMSA-BCS reconstructed profiles

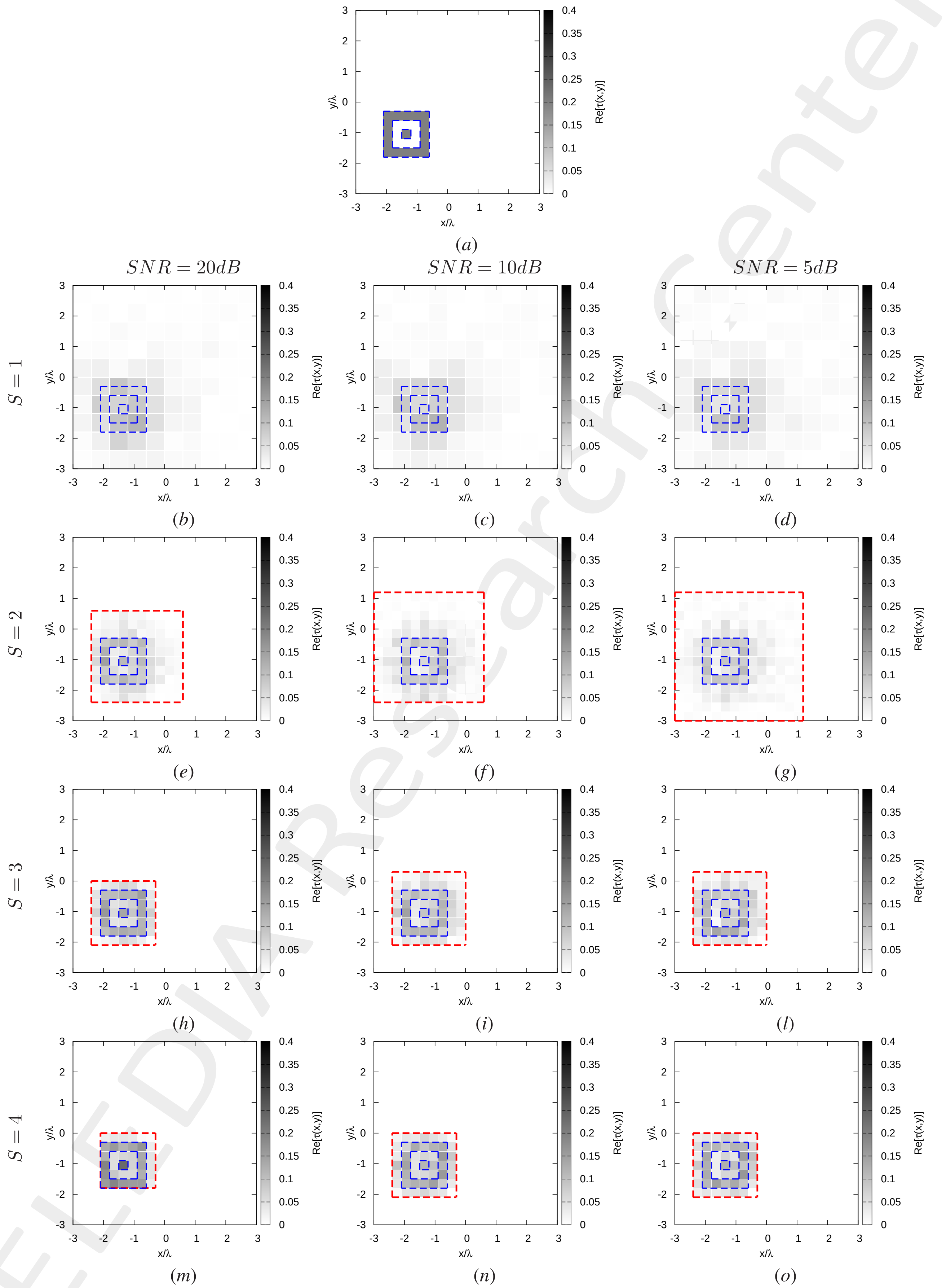

Figure 2: *Hollow Square*, $\ell = 1.5\lambda$, $\tau = 0.20$ - (a) Actual profile and (b)-(o) IMSA-BCS reconstructed profiles for $(b)(e)(h)(m)$ $SNR = 20$ [dB], $(c)(f)(i)(n)$ $SNR = 10$ [dB] and $(d)(g)(l)(o)$ $SNR = 5$ [dB] at the step (b)-(d) $S = 1$, (e)-(g) $S = 2$, (h)-(l) $S = 3$ and (m)-(o) $S = 4$.

	$SNR = 50dB$			
	$S = 1$	$S = 2$	$S = 3$	$S = 4$
ξ_{tot}	1.67×10^{-2}	8.31×10^{-3}	5.77×10^{-3}	4.48×10^{-3}
ξ_{int}	1.02×10^{-1}	8.40×10^{-2}	5.73×10^{-2}	4.44×10^{-2}
ξ_{ext}	1.22×10^{-2}	4.75×10^{-3}	3.29×10^{-3}	2.54×10^{-3}
	$SNR = 20dB$			
	$S = 1$	$S = 2$	$S = 3$	$S = 4$
ξ_{tot}	1.65×10^{-2}	8.30×10^{-3}	6.14×10^{-3}	3.98×10^{-3}
ξ_{int}	9.89×10^{-2}	8.34×10^{-2}	6.08×10^{-2}	4.05×10^{-2}
ξ_{ext}	1.20×10^{-2}	4.74×10^{-3}	3.59×10^{-3}	2.23×10^{-3}
	$SNR = 10dB$			
	$S = 1$	$S = 2$	$S = 3$	$S = 4$
ξ_{tot}	1.67×10^{-2}	9.62×10^{-3}	7.83×10^{-3}	6.72×10^{-3}
ξ_{int}	1.00×10^{-1}	9.62×10^{-2}	7.86×10^{-2}	6.62×10^{-2}
ξ_{ext}	1.21×10^{-2}	5.42×10^{-3}	4.53×10^{-3}	3.99×10^{-3}
	$SNR = 5dB$			
	$S = 1$	$S = 2$	$S = 3$	$S = 4$
ξ_{tot}	1.82×10^{-2}	1.02×10^{-2}	8.06×10^{-3}	6.82×10^{-3}
ξ_{int}	1.08×10^{-1}	9.66×10^{-2}	7.97×10^{-2}	6.62×10^{-2}
ξ_{ext}	1.27×10^{-2}	5.76×10^{-3}	4.59×10^{-3}	4.02×10^{-3}

Table III: *Hollow Square*, $\ell = 1.5\lambda$, $\tau = 0.20$ - Reconstrution errors: total (ξ_{tot}), internal (ξ_{int}) and external (ξ_{ext}) errors.

	$SNR = 50dB$			
	$S = 1$	$S = 2$	$S = 3$	$S = 4$
$L^{(S)}$	6.00	1.80	1.50	1.50
$N^{(S)}$	100	175	175	175
$Q^{(S)}$	100	100	49	36
	$SNR = 20dB$			
	$S = 1$	$S = 2$	$S = 3$	$S = 4$
$L^{(S)}$	6.00	1.80	1.50	1.50
$N^{(S)}$	100	175	175	175
$Q^{(S)}$	100	100	49	36
	$SNR = 10dB$			
	$S = 1$	$S = 2$	$S = 3$	$S = 4$
$L^{(S)}$	6.00	2.10	2.10	2.10
$N^{(S)}$	100	208	208	208
$Q^{(S)}$	100	144	64	49
	$SNR = 5dB$			
	$S = 1$	$S = 2$	$S = 3$	$S = 4$
$L^{(S)}$	6.00	2.10	2.10	2.10
$N^{(S)}$	100	247	247	247
$Q^{(S)}$	100	196	64	49

Table IV: *Hollow Square*, $\ell = 1.5\lambda$, $\tau = 0.20$ - Investigation domain parameters: restricted investigation domain size $L^{(S)}$, total number of cells $N^{(S)}$ and number of cells within the restricted domain size $Q^{(S)}$.

1.0.3 Hollow Square, $\ell = 1.5\lambda$, $\tau = 0.25$ - IMSA-BCS reconstructed profiles

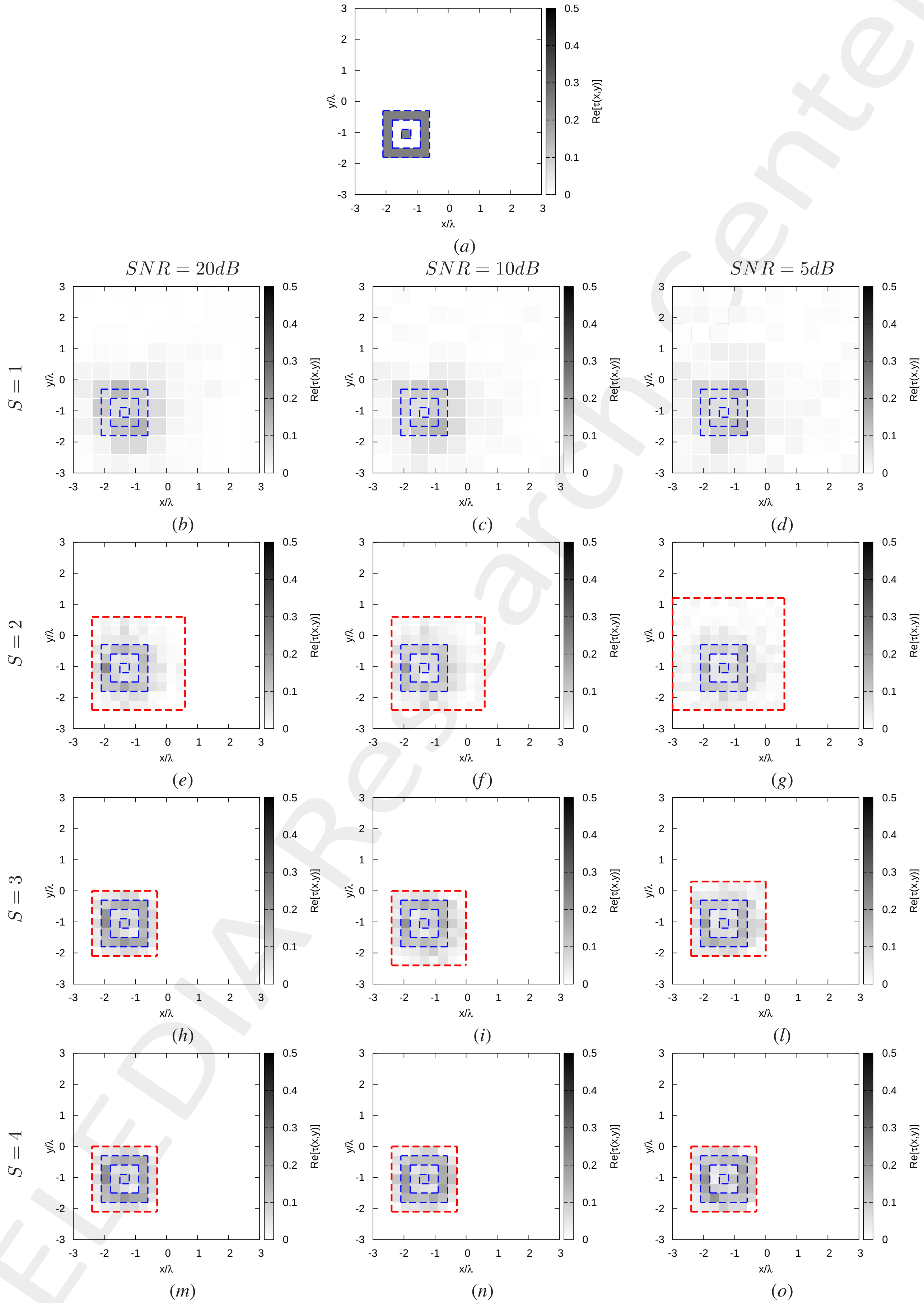

Figure 3: *Hollow Square*, $\ell = 1.5\lambda$, $\tau = 0.25$ - (a) Actual profile and (b)-(o) IMSA-BCS reconstructed profiles for $(b)(e)(h)(m)$ $SNR = 20$ [dB], $(c)(f)(i)(n)$ $SNR = 10$ [dB] and $(d)(g)(l)(o)$ $SNR = 5$ [dB] at the step (b)-(d) $S = 1$, (e)-(g) $S = 2$, (h)-(l) $S = 3$ and (m)-(o) $S = 4$.

	$SNR = 50dB$			
	$S = 1$	$S = 2$	$S = 3$	$S = 4$
ξ_{tot}	2.12×10^{-2}	9.78×10^{-3}	7.40×10^{-3}	7.40×10^{-3}
ξ_{int}	1.19×10^{-1}	9.96×10^{-2}	7.43×10^{-2}	7.43×10^{-2}
ξ_{ext}	1.57×10^{-2}	5.51×10^{-3}	4.22×10^{-3}	4.22×10^{-3}
	$SNR = 20dB$			
	$S = 1$	$S = 2$	$S = 3$	$S = 4$
ξ_{tot}	2.08×10^{-2}	1.06×10^{-2}	7.66×10^{-3}	7.66×10^{-3}
ξ_{int}	1.14×10^{-1}	1.05×10^{-1}	7.49×10^{-2}	7.49×10^{-2}
ξ_{ext}	1.55×10^{-2}	6.10×10^{-3}	4.45×10^{-3}	4.45×10^{-3}
	$SNR = 10dB$			
	$S = 1$	$S = 2$	$S = 3$	$S = 4$
ξ_{tot}	2.09×10^{-2}	1.14×10^{-2}	9.76×10^{-3}	8.52×10^{-3}
ξ_{int}	1.18×10^{-1}	1.12×10^{-1}	9.53×10^{-2}	8.31×10^{-2}
ξ_{ext}	1.53×10^{-2}	6.61×10^{-3}	5.74×10^{-3}	5.00×10^{-3}
	$SNR = 5dB$			
	$S = 1$	$S = 2$	$S = 3$	$S = 4$
ξ_{tot}	2.32×10^{-2}	1.27×10^{-2}	1.01×10^{-2}	9.14×10^{-3}
ξ_{int}	1.23×10^{-1}	1.21×10^{-1}	1.00×10^{-1}	8.62×10^{-2}
ξ_{ext}	1.68×10^{-2}	7.20×10^{-3}	5.81×10^{-3}	5.42×10^{-3}

Table V: *Hollow Square*, $\ell = 1.5\lambda$, $\tau = 0.25$ - Reconstrution errors: total (ξ_{tot}), internal (ξ_{int}) and external (ξ_{ext}) errors.

	$SNR = 50dB$			
	$S = 1$	$S = 2$	$S = 3$	$S = 4$
$L^{(S)}$	6.00	2.10	2.10	2.10
$N^{(S)}$	100	175	175	175
$Q^{(S)}$	100	100	49	49
	$SNR = 20dB$			
	$S = 1$	$S = 2$	$S = 3$	$S = 4$
$L^{(S)}$	6.00	2.10	2.10	2.10
$N^{(S)}$	100	175	175	175
$Q^{(S)}$	100	100	49	49
	$SNR = 10dB$			
	$S = 1$	$S = 2$	$S = 3$	$S = 4$
$L^{(S)}$	6.00	2.10	2.10	2.10
$N^{(S)}$	100	175	175	175
$Q^{(S)}$	100	100	64	49
	$SNR = 5dB$			
	$S = 1$	$S = 2$	$S = 3$	$S = 4$
$L^{(S)}$	6.00	2.10	2.10	2.10
$N^{(S)}$	100	208	208	208
$Q^{(S)}$	100	144	64	49

Table VI: *Hollow Square*, $\ell = 1.5\lambda$, $\tau = 0.25$ - Investigation domain parameters: restricted investigation domain size $L^{(S)}$, total number of cells $N^{(S)}$ and number of cells within the restricted domain size $Q^{(S)}$.

1.0.4 Hollow Square, $\ell = 1.5\lambda$, $\tau = 1.00$ - IMSA-BCS reconstructed profiles

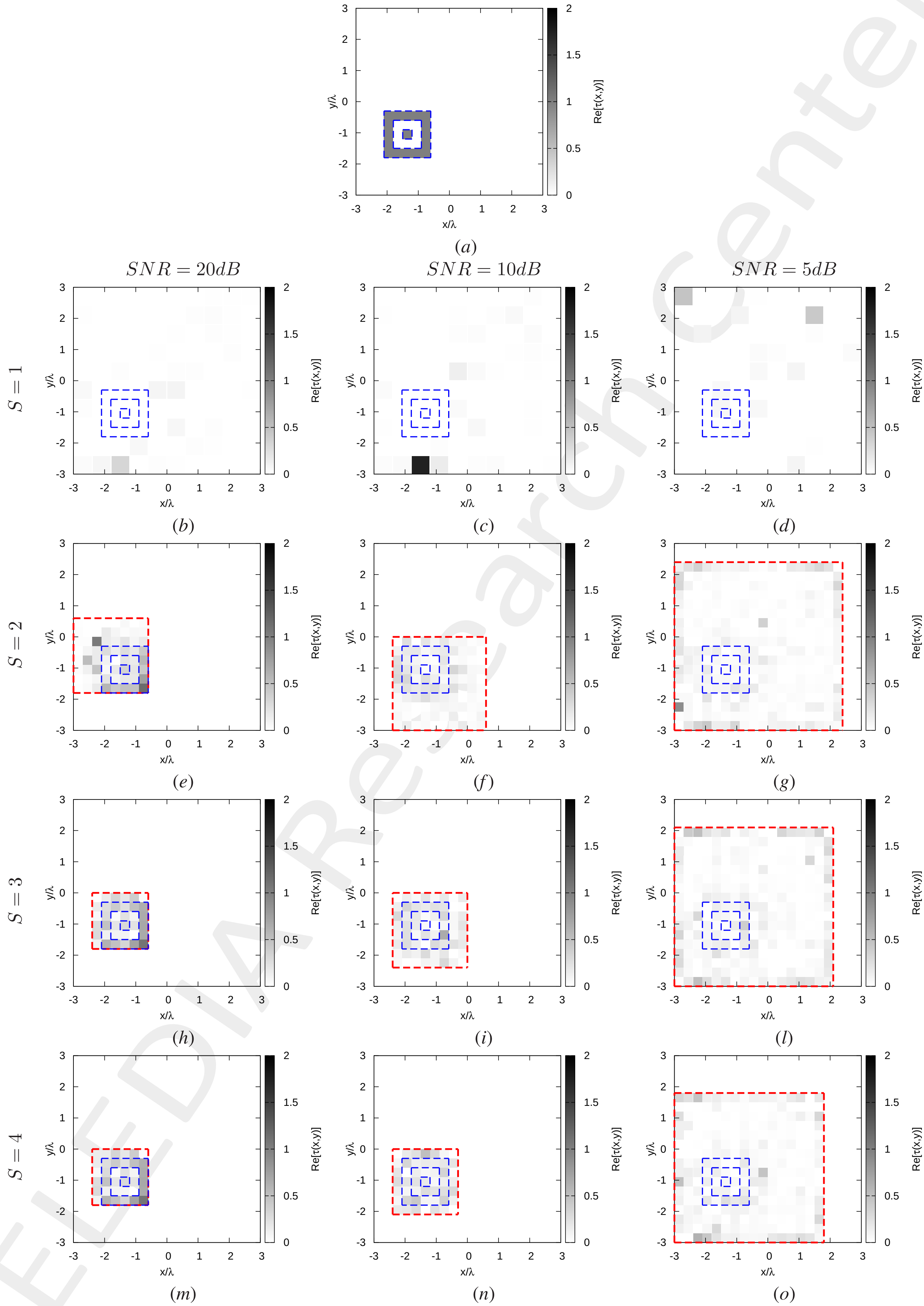

Figure 4: *Hollow Square*, $\ell = 1.5\lambda$, $\tau = 1.00$ - (a) Actual profile and (b)-(o) IMSA-BCS reconstructed profiles for $(b)(e)(h)(m)$ $SNR = 20$ [dB], $(c)(f)(i)(n)$ $SNR = 10$ [dB] and $(d)(g)(l)(o)$ $SNR = 5$ [dB] at the step (b)-(d) $S = 1$, (e)-(g) $S = 2$, (h)-(l) $S = 3$ and (m)-(o) $S = 4$.

	$SNR = 50dB$			
	$S = 1$	$S = 2$	$S = 3$	$S = 4$
ξ_{tot}	7.26×10^{-2}	5.04×10^{-2}	2.69×10^{-2}	4.95×10^{-2}
ξ_{int}	5.96×10^{-1}	3.76×10^{-1}	4.09×10^{-1}	4.11×10^{-1}
ξ_{ext}	3.22×10^{-2}	2.43×10^{-2}	5.30×10^{-3}	2.48×10^{-2}
	$SNR = 20dB$			
	$S = 1$	$S = 2$	$S = 3$	$S = 4$
ξ_{tot}	6.77×10^{-2}	3.01×10^{-2}	2.00×10^{-2}	2.00×10^{-2}
ξ_{int}	5.67×10^{-1}	3.08×10^{-1}	2.57×10^{-1}	2.57×10^{-1}
ξ_{ext}	3.36×10^{-2}	1.41×10^{-2}	7.76×10^{-3}	7.76×10^{-3}
	$SNR = 10dB$			
	$S = 1$	$S = 2$	$S = 3$	$S = 4$
ξ_{tot}	9.05×10^{-2}	1.33×10^{-1}	1.33×10^{-1}	1.33×10^{-1}
ξ_{int}	5.79×10^{-1}	5.00×10^{-1}	5.00×10^{-1}	5.00×10^{-1}
ξ_{ext}	5.27×10^{-2}	1.05×10^{-1}	1.05×10^{-1}	1.05×10^{-1}
	$SNR = 5dB$			
	$S = 1$	$S = 2$	$S = 3$	$S = 4$
ξ_{tot}	1.27×10^{-1}	8.22×10^{-2}	7.76×10^{-2}	7.17×10^{-2}
ξ_{int}	5.33×10^{-1}	4.56×10^{-1}	4.53×10^{-1}	4.47×10^{-1}
ξ_{ext}	8.70×10^{-2}	4.74×10^{-2}	4.75×10^{-2}	4.26×10^{-2}

Table VII: *Hollow Square*, $\ell = 1.5\lambda$, $\tau = 1.00$ - Reconstrution errors: total (ξ_{tot}), internal (ξ_{int}) and external (ξ_{ext}) errors.

	$SNR = 50dB$			
	$S = 1$	$S = 2$	$S = 3$	$S = 4$
$L^{(S)}$	6.00	3.30	2.25	3.30
$N^{(S)}$	100	127	127	127
$Q^{(S)}$	100	36	23	63
	$SNR = 20dB$			
	$S = 1$	$S = 2$	$S = 3$	$S = 4$
$L^{(S)}$	6.00	1.80	1.80	1.80
$N^{(S)}$	100	148	148	148
$Q^{(S)}$	100	64	36	36
	$SNR = 10dB$			
	$S = 1$	$S = 2$	$S = 3$	$S = 4$
$L^{(S)}$	6.00	2.40	2.40	2.40
$N^{(S)}$	100	148	148	148
$Q^{(S)}$	100	64	64	64
	$SNR = 5dB$			
	$S = 1$	$S = 2$	$S = 3$	$S = 4$
$L^{(S)}$	6.00	4.80	4.20	4.20
$N^{(S)}$	100	343	343	343
$Q^{(S)}$	100	324	289	256

Table VIII: *Hollow Square*, $\ell = 1.5\lambda$, $\tau = 1.00$ - Investigation domain parameters: restricted investigation domain size $L^{(S)}$, total number of cells $N^{(S)}$ and number of cells within the restricted domain size $Q^{(S)}$.

1.0.5 Hollow Square, $\ell = 1.5\lambda$ - Resume: Errors vs. τ

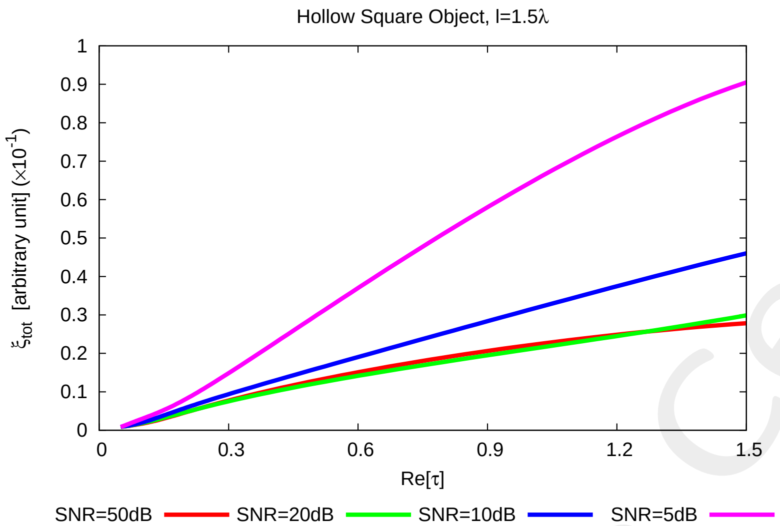

(a)

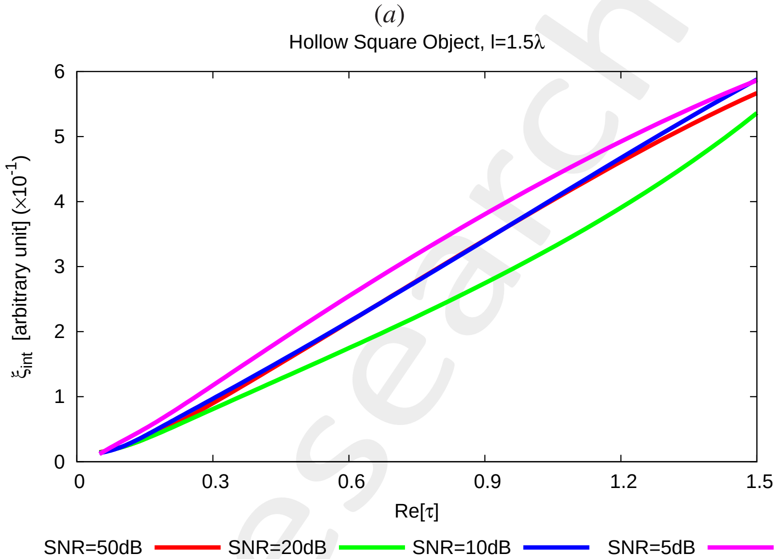

(b)

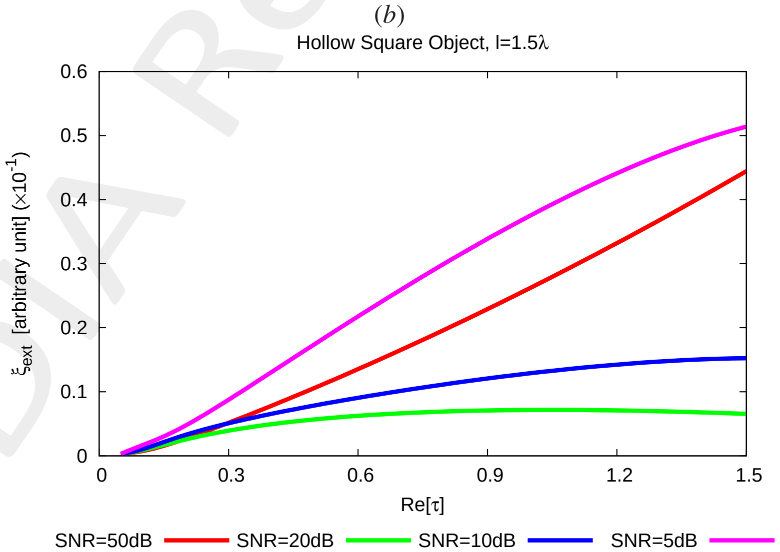

(c)

Figure 5: *Hollow Square*, $\ell = 1.5\lambda$ - Reconstruction errors vs. τ: (a) total error, (b) internal error and (c) external error.

1.0.6 Hollow Square, $\ell = 1.5\lambda$ - Resume: Errors vs. $IMSA$ step, S

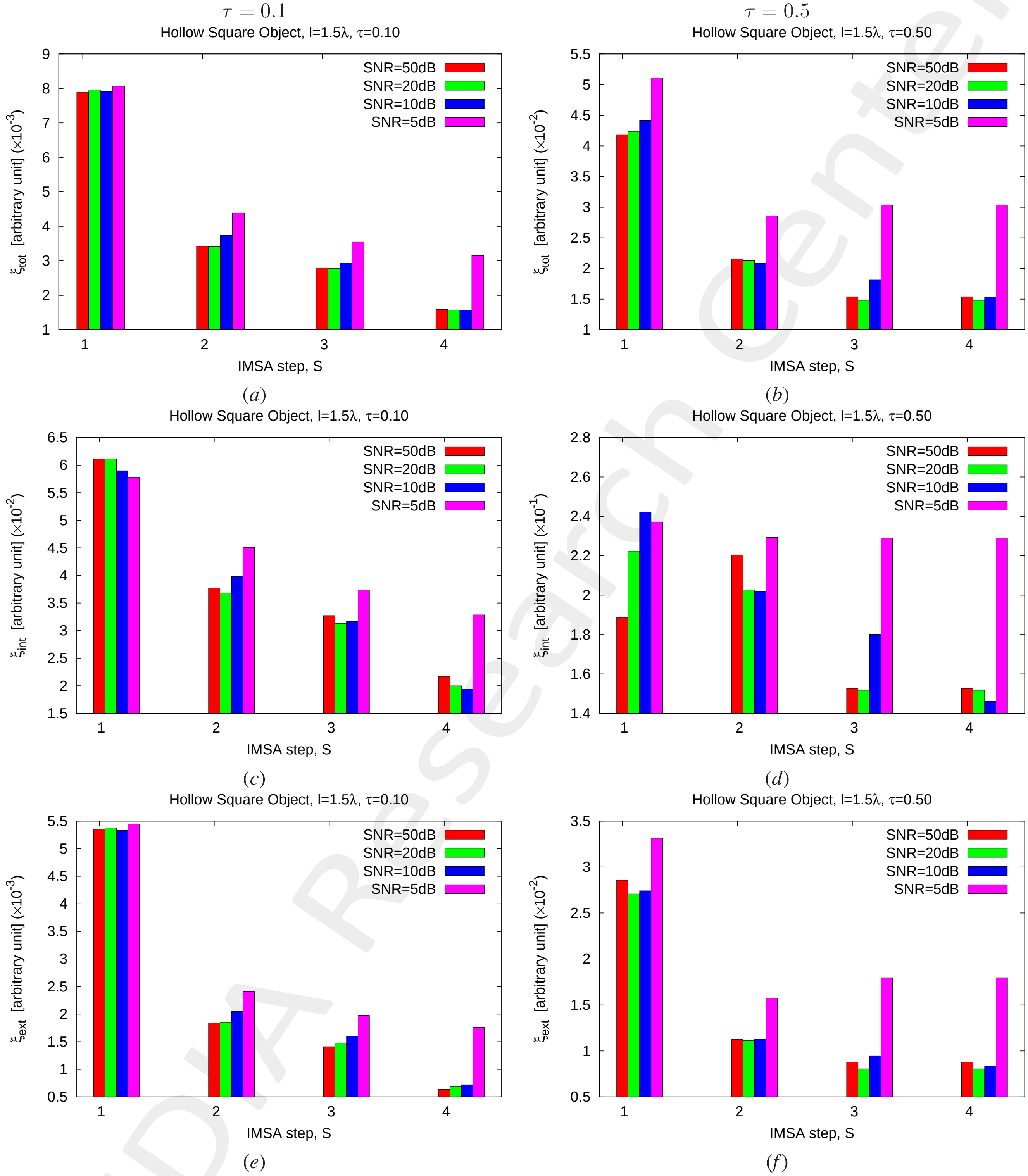

Figure 6: *Hollow Square*, $\ell = 1.5\lambda$ - Reconstruction errors vs. $IMSA$ step, S: $(a)(b)$ total error, $(c)(d)$ internal error and $(e)(f)$ external error for $(a)(c)(e)$ $\tau = 0.1$ and $(b)(d)(f)$ $\tau = 0.5$.

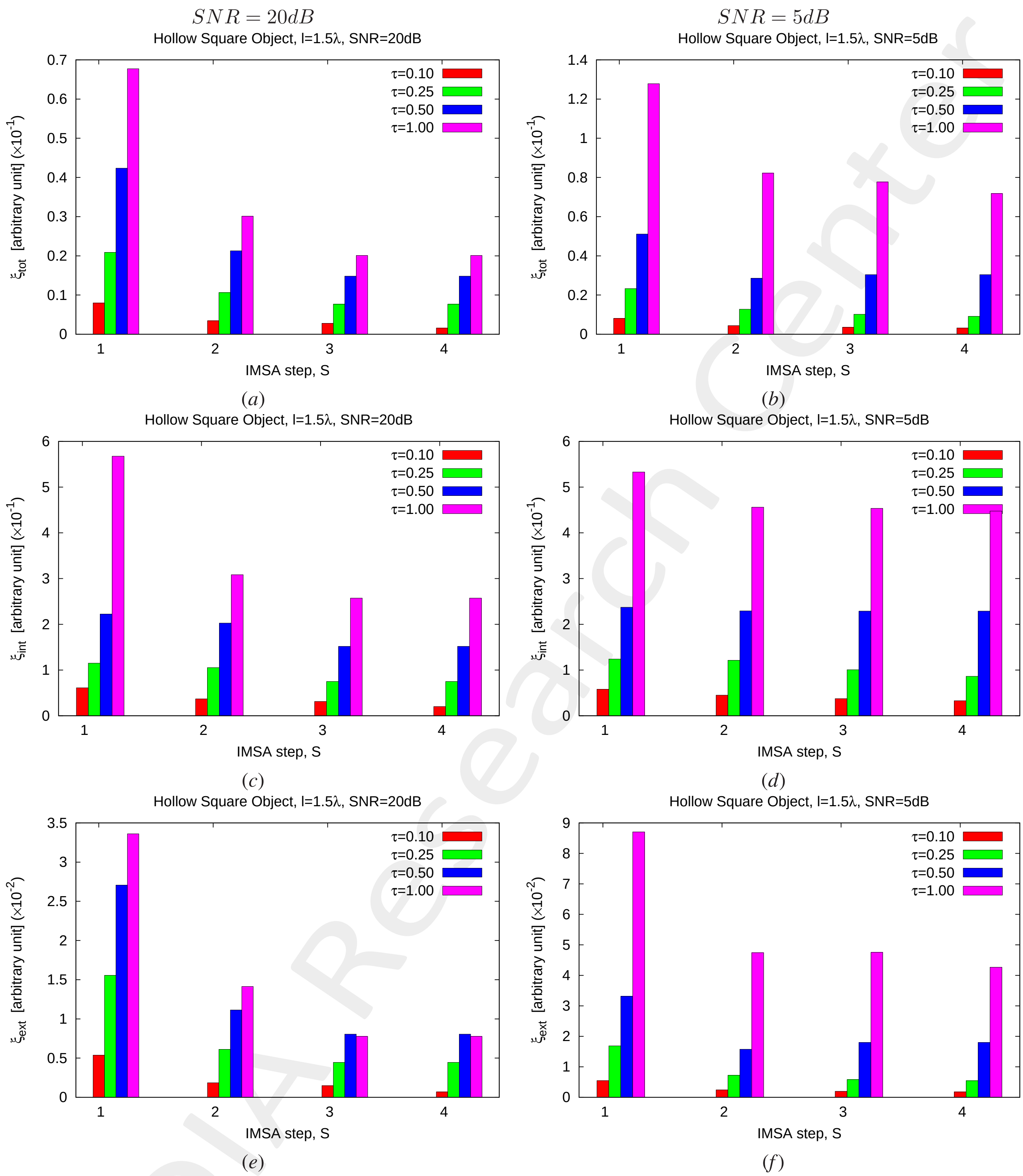

Figure 7: *Hollow Square*, $\ell = 1.5\lambda$ - Reconstruction errors vs. $IMSA$ step, S: $(a)(b)$ total error, $(c)(d)$ internal error and $(e)(f)$ external error for $(a)(c)(e)$ $SNR = 10dB$ and $(b)(d)(f)$ $SNR = 5dB$.

More information on the topics of this document can be found in the following list of references.

References

[1] G. Oliveri, M. Salucci, N. Anselmi, and A. Massa, "Compressive sensing as applied to inverse problems for imaging: theory, applications, current trends, and open challenges," *IEEE Antennas Propag. Mag. - Special Issue on 'Electromagnetic Inverse Problems for Sensing and Imaging,'* vol. 59, no. 5, pp. 34-46, Oct. 2017 (DOI: 10.1109/MAP.2017.2731204).

[2] A. Massa, P. Rocca, and G. Oliveri, "Compressive sensing in electromagnetics - A review," *IEEE Antennas Propag. Mag.*, pp. 224-238, vol. 57, no. 1, Feb. 2015 (DOI: 10.1109/MAP.2015.2397092).

[3] A. Massa and F. Texeira, "Guest-Editorial: Special Cluster on Compressive Sensing as Applied to Electromagnetics," *IEEE Antennas Wirel. Propag. Lett.*, vol. 14, pp. 1022-1026, 2015 (DOI: 10.1109/LAWP.2015.2425011).

[4] M. Salucci, L. Poli, F. Zardi, L. Tosi, S. Lusa, and A. Massa, "Contrast source inversion of sparse targets through multi-resolution Bayesian compressive sensing," *Inverse Probl.*, vol. 40, no. 5, p. 055016, May 2024 (DOI 10.1088/1361-6420/ad3b33).

[5] G. Oliveri, N. Anselmi, M. Salucci, L. Poli, and A. Massa, "Compressive sampling-based scattering data acquisition in microwave imaging," *J. Electromagn. Waves Appl.* J, vol. 37, no. 5, 693-729, Mar. 2023 (DOI: 10.1080/09205071.2023.2188263).

[6] G. Oliveri, L. Poli, N. Anselmi, M. Salucci, and A. Massa, "Compressive sensing-based Born iterative method for tomographic imaging," *IEEE Tran. Microw. Theory Techn.*, vol. 67, no. 5, pp. 1753-1765, May 2019 (DOI: 10.1109/TMTT.2019.2899848).

[7] M. Salucci, L. Poli, and G. Oliveri, "Full-vectorial 3D microwave imaging of sparse scatterers through a multi-task Bayesian compressive sensing approach," *Journal of Imaging*, vol. 5, no. 1, pp. 1-24, Jan. 2019 (DOI: 10.3390/jimaging5010019).

[8] M. Salucci, A. Gelmini, L. Poli, G. Oliveri, and A. Massa, "Progressive compressive sensing for exploiting frequency-diversity in GPR imaging," *J. Electromagn. Waves Appl. J*, vol. 32, no. 9, pp. 1164-1193, 2018 (DOI: 10.1080/09205071.2018.1425160).

[9] N. Anselmi, L. Poli, G. Oliveri, and A. Massa, "Iterative multi-resolution bayesian CS for microwave imaging," *IEEE Trans. Antennas Propag.*, vol. 66, no. 7, pp. 3665-3677, Jul. 2018 (DOI: 10.1109/TAP.2018.2826574).

[10] N. Anselmi, G. Oliveri, M. A. Hannan, M. Salucci, and A. Massa, "Color compressive sensing imaging of arbitrary-shaped scatterers," *IEEE Trans. Microw. Theory Techn.*, vol. 65, no. 6, pp. 1986-1999, Jun. 2017 (DOI: 10.1109/TMTT.2016.2645570).

[11] N. Anselmi, G. Oliveri, M. Salucci, and A. Massa, "Wavelet-based compressive imaging of sparse targets," *IEEE Trans. Antennas Propag.*, vol. 63, no. 11, pp. 4889-4900, Nov. 2015 (DOI: 10.1109/TAP.2015.2444423).

[12] G. Oliveri, P.-P. Ding, and L. Poli, “3D crack detection in anisotropic layered media through a sparseness-regularized solver,” *IEEE Antennas Wirel. Propag. Lett.*, vol. 14, pp. 1031-1034, 2015 (DOI: 10.1109/LAWP.2014.2365523).

[13] L. Poli, G. Oliveri, P.-P. Ding, T. Moriyama, and A. Massa, “Multifrequency Bayesian compressive sensing methods for microwave imaging,” *J. Opt. Soc. Am. A*, vol. 31, no. 11, pp. 2415-2428, 2014 (DOI: 10.1364/JOSAA.31.002415).

[14] G. Oliveri, N. Anselmi, and A. Massa, “Compressive sensing imaging of non-sparse 2D scatterers by a total-variation approach within the Born approximation,” *IEEE Trans. Antennas Propag.*, vol. 62, no. 10, pp. 5157-5170, Oct. 2014 (DOI: 10.1109/TAP.2014.2344673).